

Magnetic correlation in the square-lattice spin system (CuBr)Sr₂Nb₃O₁₀: A neutron diffraction study

S. M. Yusuf* and A. K. Bera

Solid State Physics Division, Bhabha Atomic Research Centre, Mumbai 400 085, INDIA

C. Ritter

*Institut Laue-Langevin, Boite Postale 156, 38042 Grenoble Cedex, France*Yoshihiro Tsujimoto^{1,2}, Yoshitami Ajiro¹, and Hiroshi Kageyama¹¹*Department of Energy and Hydrocarbon Chemistry, Graduate School of Engineering, Kyoto University, Nishikyo, Kyoto 615-8510, Japan*²*International Center for Materials Nanoarchitectonics, National Institute for Materials Science, Namiki 1-1, Tsukuba, Ibaraki 305-0044, Japan*

J. Paul Attfield

Centre for Science at Extreme Conditions and School of Chemistry, University of Edinburgh, Edinburgh EH9 3JZ, UK

(Received 18 February 2011; revised manuscript received 18 July 2011; published 18 August 2011)

Magnetic correlation in the quantum $S = 1/2$ square-lattice system (CuBr)Sr₂Nb₃O₁₀ has been studied by neutron diffraction. A novel commensurate in-plane, helical antiferromagnetic (AFM) ordering, characterized by the propagation vector $k = (0 \ 3/8 \ 1/2)$, has been confirmed from the appearance of magnetic Bragg peaks below $T_N \sim 7.5$ K. The ordered moment at 2 K is found to be $0.79(7) \mu_B/\text{Cu}^{2+}$ -ion. The observed helical AFM structure differs from the ground state predicted theoretically from the J_1 - J_2 model as well as from experimentally reported states for other quantum $S = 1/2$ square-lattice systems. However, the observed helical magnetic structure can be described in a J_1 - J_2 - J_3 model. Under a 4.5 T magnetic field, the spin-order changes drastically and is characterized by the propagation vector $k_1 = (0 \ 1/3 \ 0.446)$ and a probable $k_2 = (0 \ 0 \ 0)$ vector.

DOI: [10.1103/PhysRevB.84.064407](https://doi.org/10.1103/PhysRevB.84.064407)

PACS number(s): 75.47.Lx, 75.10.Jm, 75.25.-j

I. INTRODUCTION

Low-dimensional magnetic systems have been of great interest in recent years due to their unconventional, novel, and complex magnetic properties.^{1,2} Different topologies of spin arrangements such as quasi-one-dimensional spin chains, triangular, kagome, and square lattices can be found. The spin-1/2 Heisenberg square-lattice systems where magnetic moments on a square lattice are subjected to the nearest-neighbor interaction J_1 along the side of the square and the next-nearest-neighbor interaction J_2 along the diagonal of the square have received considerable attention. In the literature a large number of theoretical studies on systems with antiferromagnetic (AFM) J_1 and J_2 exist.³⁻¹⁴ Here the J_1 - J_2 model³⁻¹⁴ reveals several interesting magnetic ground states involving quantum phase transitions, such as (i) for $\alpha (=|J_2/J_1|) \lesssim 0.4$, a Néel AFM state [$Q = (\pi \ \pi)$], (ii) for $\alpha \sim 0.4$ - 0.6 , a quantum spin-liquid state, and (iii) for $\alpha \gtrsim 0.6$, an ordered collinear AFM state [$Q = (\pi \ 0)$ or $(0 \ \pi)$], i.e., AFM coupling of ferromagnetic (FM) chains in a given plane (by disorder stabilization). However, for the model with FM J_1 and AFM J_2 , so far only a few studies exist.¹⁵⁻¹⁹ The FM J_1 - J_2 model yields a FM ground state [$Q = (0 \ 0)$] for lower values of $\alpha \lesssim 0.4$. However, the FM state breaks down at $\alpha \sim 0.4$. For the sufficiently large J_2 ($\alpha \gtrsim 0.6$), a long-ranged collinear stripe phase, similar to the finding for the corresponding AFM J_1 - J_2 model, appears. A disordered state is predicted over the intermediate regime of α . The precise nature of the disordered state is qualitatively different for the FM J_1 from AFM J_1 . While the model with the AFM J_1 has a spin-liquid ground state for a narrow range

of α ,¹⁴ the intermediate state of the model with the FM J_1 is either a spin nematic¹⁵ or presumably does not exist at all.¹⁶ Extensive experimental investigations, carried out on a number of vanadium-based square-lattice compounds Li₂VOSiO₄ and Li₂VOGeO₄, reveal AFM J_1 and J_2 .²⁰ The AFM J_1 and J_2 have also been found for other systems, such as the two-dimensional (2D) square-lattice antiferromagnet Cu(pz)₂(ClO₄)₂ (where pz denotes pyrazine),²¹ VOMoO₄,²² and the layered perovskite PbVO₃.^{23,24} The square-lattice layered vanadium phosphate AA'VO(PO₄)₂ with AA' = Zn₂ also reveals AFM J_1 and J_2 .^{25,26} On the other hand, the other layered vanadium phosphates AA'VO(PO₄)₂ with AA' = Pb₂,²⁷ BaZn,²⁸ SrZn,²⁹ and BaCd³⁰ (with square-lattice spin arrangements) show the FM J_1 and AFM J_2 . A recent investigation shows that PbZnVO(PO₄)₂ also belongs to the square-lattice compound with FM J_1 and AFM J_2 .³¹ A preliminary magnetization and specific-heat study³² has suggested that the triple-layered perovskite (CuBr)Sr₂Nb₃O₁₀ is a possible new addition to the list with the FM J_1 and AFM J_2 .

(CuBr)Sr₂Nb₃O₁₀ belongs to the Dion-Jacobson series of layered oxides with the general formula (CuX)A_{n-1}B_nO_{3n+1}, where X = Br⁻, Cl⁻ ions, A = La³⁺, Ca²⁺, Na⁺ ions, and B = Nb⁵⁺, Ta⁵⁺, and Ti⁴⁺ ions.³²⁻³⁶ This system shows a layered-type crystal structure (tetragonal symmetry, space group $P4/mmm$) with $a = 3.91069(4)$ and $c = 16.0207(3)$ Å. CuBr square planes are widely separated by nonmagnetic slabs of [Sr₂Nb₃O₁₀]⁻ along the crystallographic c axis. The $S = 1/2$ Cu ions are octahedrally coordinated by two apical oxygen atoms and by four bromine atoms. Magnetization (M) and specific-heat studies^{32,33} suggested that this compound

is a geometrically frustrated quantum spin system in which the square-lattice arrangement of the Cu ions causes spin frustration due to the competing AFM and FM interactions. Two successive phase transitions at $T_{c1} \sim 9.3$ and $T_{c2} \sim 7.5$ K were observed in the specific-heat study³² and were found to merge under an applied magnetic field (H) of 3 T. The magnetic specific heat C_m has a T^2 dependence below 5 K ($< T_{c2}$), which is a characteristic feature of 2D AFM spin correlations. A 1/3 plateau of the saturated magnetization was observed in the M vs H curves as a metamagnetic transition at low temperatures. The gradual deviation of magnetic susceptibility from Curie-Weiss behavior below 100 K suggested a short-range spin-spin correlation within the CuBr plane is already well developed at high temperatures.^{32,33}

Prompted by these interesting magnetization and specific-heat results, we have performed neutron diffraction experiments using a powder sample of $(\text{CuBr})\text{Sr}_2\text{Nb}_3\text{O}_{10}$ to gain a microscopic understanding of the nature of magnetic ground state of this interesting square-lattice spin system. An in-plane (in the ab plane) helical AFM structure has been discovered from the appearance of additional magnetic Bragg peaks, indexed with the propagation vector $k = (0\ 3/8\ 1/2)$, in contrast to the theoretically predicted and experimentally reported magnetic ground states for other $S = 1/2$ square-lattice systems. A different magnetic order, characterized by the propagation vector $k_1 = (0\ 1/3\ 0.446)$ and a probable $k_2 = (0\ 0\ 0)$ vector, has been observed under a 4.5 T magnetic field. The observed magnetic structures show that $(\text{CuBr})\text{Sr}_2\text{Nb}_3\text{O}_{10}$ belongs to a new class of the spin-1/2 square-lattice system.

II. EXPERIMENTAL

The polycrystalline sample of $(\text{CuBr})\text{Sr}_2\text{Nb}_3\text{O}_{10}$ was prepared by a two-step-process involving the solid-state synthesis to yield $\text{RbSr}_2\text{Nb}_3\text{O}_{10}$ followed by a low-temperature ion-exchange reaction by CuBr_2 as described elsewhere.³³ High-intensity neutron diffraction patterns were recorded at 2, 5, 8, 12, and 26 K using the D20 powder neutron diffractometer, at the Institute Laue Langevin, Grenoble, France, with a wavelength of $\lambda = 2.418$ Å. For these measurements, the sample was placed in a vanadium can, and an orange cryostat was used for low-temperature measurements. Additional data were taken between 2 and 12 K under an applied magnetic field of up to 4.5 T using a cryomagnet. The diffraction data were analyzed by the Rietveld method using the FULLPROF program.^{37,38} The representation theory analysis was performed using the BASIREPS software for the determination of magnetic structure.^{37,38}

III. RESULTS AND DISCUSSION

The neutron diffraction pattern of $(\text{CuBr})\text{Sr}_2\text{Nb}_3\text{O}_{10}$ at 26 K (paramagnetic state) is shown in Fig. 1. The Rietveld analysis of the pattern confirms the tetragonal crystal structure shown in Fig. 2 with space group $P4/mmm$. The refined values of the lattice constants $a = 3.888(1)$ Å and $c = 15.947(1)$ Å are in good agreement with the values reported earlier from an x-ray diffraction study.^{32,33} The values of other crystal structure parameters, such as fractional atomic coordinates,

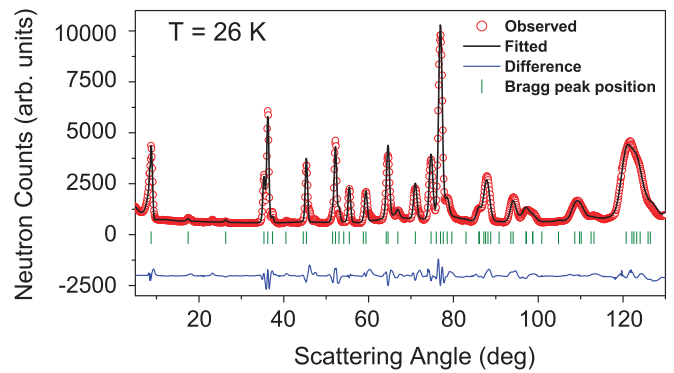


FIG. 1. (Color online) The observed (open circles), calculated (solid lines) and difference neutron diffraction patterns for $(\text{CuBr})\text{Sr}_2\text{Nb}_3\text{O}_{10}$ at 26 K (paramagnetic state). The vertical bars show the nuclear Bragg peak positions.

bond lengths, and bond angles, are also in a good agreement with the previously reported values from an x-ray diffraction study and are not reported here. No structural change has been observed down to the lowest measured temperature 2 K. It may be mentioned that Tassel *et al.*³⁹ and independently Tsirlin *et al.*⁴⁰ reported the existence of a very small orthorhombic distortion in the similar compound $(\text{CuCl})\text{LaNb}_2\text{O}_7$, which belongs to the Dion-Jacobson series with $n = 2$. Due to the limited resolution available at D20, we cannot exclude the existence of such a distortion in $(\text{CuBr})\text{Sr}_2\text{Nb}_3\text{O}_{10}$. The magnetic diffraction patterns at 8, 5, and 2 K, after subtraction of the 26 K nuclear data, are shown in Fig. 3. At 2 and 5 K, the appearance of additional weak magnetic Bragg peaks confirms a long-range AFM ordering in this compound. At 8 K, no magnetic peaks are observed, in agreement with the earlier dc magnetization study in which M vs T curves showed a single magnetic transition at ~ 7.5 K (T_N).³² However, two successive magnetic phase transitions at 9.3 (T_{c1}) and 7.5 (T_{c2}) K were observed in the specific-heat curve.³² The observed magnetic ordering in the present neutron diffraction study thus can be assigned to the “second” magnetic transition temperature $T_{c2} = 7.5$ K. In the present neutron diffraction study, no signature of static spin-spin correlation has been found at 8 K, i.e., ($T_{c2} \leq T \leq T_{c1}$), which is consistent with the μSR results,³³ showing the fluctuating nature of spin-spin correlations over the intermediate temperature range ($7.5 \text{ K} \leq T \leq 9.3 \text{ K}$).

All of the magnetic peaks observed at 2 and 5 K, are indexed with the propagation vector $k = (0\ 3/8\ 1/2)$. The magnetic structure has been analyzed using irreducible representational theory as described by Bertaut.^{41,42} For the propagation vector $k = (0\ 3/8\ 1/2)$, the irreducible representations of the propagation vector group G_k are given in Table I. In the space group $P4/mmm$ with the propagation vector $k = (0\ 3/8\ 1/2)$, there are three possible irreducible representations. The magnetic reducible representation Γ for $1b$ site (Cu site) can be decomposed as a direct sum of irreducible representations as

$$\Gamma_{\text{mag}} = \Gamma_1 + \Gamma_2 + \Gamma_3$$

The basis vectors of the Cu position $1b$ (0, 0, 0.5) for the representations, calculated using the projection operator technique implemented in BASIREPS,³⁸ are given in Table II.

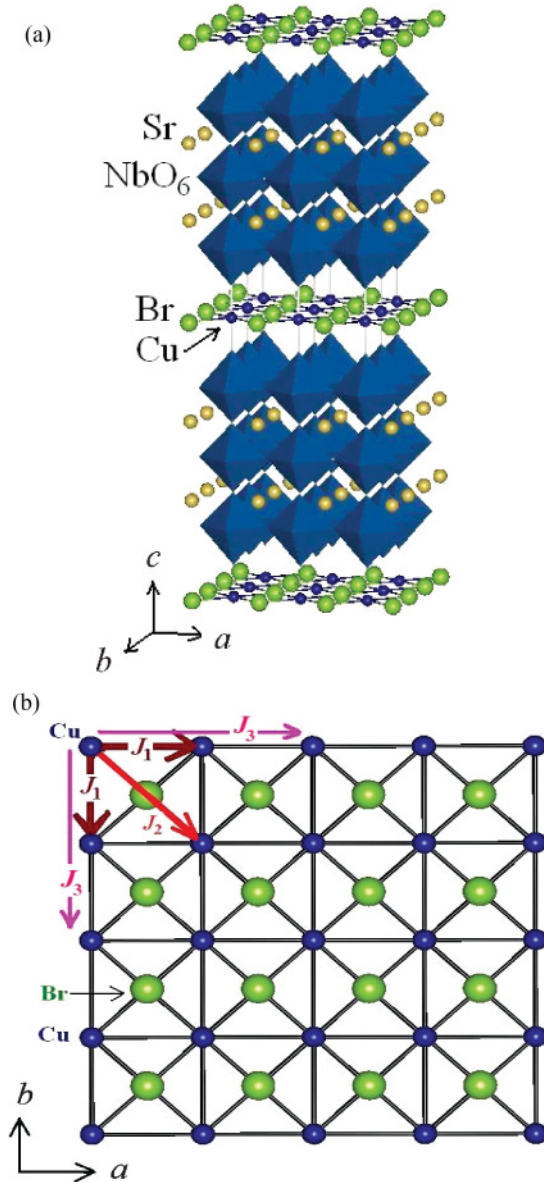


FIG. 2. (Color online) (a) The layered crystal structure of $(\text{CuBr})\text{Sr}_2\text{Nb}_3\text{O}_{10}$. (b) The square-lattice arrangement of Cu-ions in the ab plane. The pathways of nearest-neighbor, next-nearest-neighbor, and next-to-next-nearest-neighbor exchange interactions (J_1 , J_2 , and J_3 , respectively) are shown.

The best fit to the observed diffraction pattern at 2 K (giving a magnetic R factor of 3.6%) is obtained by refinement of the magnetic structure with a linear combination of the representations Γ_1 and Γ_3 . The fitted pattern is shown in Fig. 4. The corresponding magnetic structure is a helical AFM structure as shown in Fig. 5. A helix of Cu spins is formed in the ab plane and an AFM coupling of adjacent planes is found along the c axis. The Cu^{2+} moments rotate around the c axis within the ab plane as shown in Fig. 5(a), and the helix propagates along the b axis with a rotation of 135° between successive moments. The helical chains are coupled ferromagnetically along the a axis. The ordered moment is found to be $0.79(7) \mu_B/\text{Cu}^{2+}$ -ion at 2 K. The observed helical AFM structure for the present square-lattice system $(\text{CuBr})\text{Sr}_2\text{Nb}_3\text{O}_{10}$ is in contrast to the

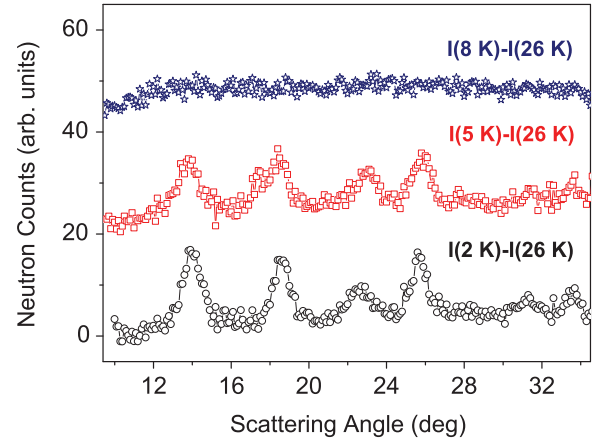


FIG. 3. (Color online) The low-angle region of the magnetic diffraction patterns for $(\text{CuBr})\text{Sr}_2\text{Nb}_3\text{O}_{10}$ at 8, 5, and 2 K after subtraction of the 26 K nuclear pattern.

reported collinear AFM structure for other square-lattice systems, such as layered vanadium phosphates $AA'\text{VO}(\text{PO}_4)_2$ with $AA' = \text{Pb}_2$,²⁷ BaZn ,²⁸ SrZn ,²⁹ PbZn ,¹⁶ and BaCd ³⁰ with the FM J_1 and AFM J_2 . A helical AFM structure is also in contrast to the theoretically predicted magnetic states for the FM J_1 - J_2 model, namely, a collinear AFM structure for values of α ($=|J_2/J_1|$) $\gtrsim 0.6$, and a FM structure for $\alpha \lesssim 0.4$.¹⁵⁻¹⁹

The role of α in $(\text{CuBr})\text{Sr}_2\text{Nb}_3\text{O}_{10}$ as well as in other square-lattice compounds may be described as follows. The α value for the present compound was found (from the earlier magnetization measurement³²) to be 0.59 [$J_2/J_1 = 30.6 \text{ K}/(-51.5 \text{ K})$] with a FM J_1 . From the value of α , it is evident that this system is at the phase boundary between ordered collinear AFM (with a dominating AFM J_2) and disordered states in the theoretical phase diagram.¹⁵⁻¹⁹ A collinear AFM structure [$Q = (\pi, 0)$ or $(0, \pi)$] was found for $(\text{CuBr})\text{LaNb}_2\text{O}_7$,⁴³ an $n = 2$ member of the present Dion-Jacobson series $[(\text{CuX})A_{n-1}B_n\text{O}_{3n+1}]$ with FM J_1 and an α value of $(J_2/J_1 = 41.3 \text{ K}/(-35.6 \text{ K})) = 1.1$, which is well inside the range for a collinear AFM state ($\alpha \gtrsim 0.6$). The other reported square-lattice compounds with FM J_1 having a collinear AFM structure, such as $\text{Pb}_2\text{VO}(\text{PO}_4)_2$ ($\alpha \sim 1.6$)²⁷ and $\text{BaCdVO}(\text{PO}_4)_2$ ($\alpha \sim 0.9$),³⁰ are as well far above the lower limit of $\alpha \gtrsim 0.6$. At the other extreme of α values [i.e., for compounds with lower values of $J_2/(\text{FM}J_1)$], a FM state [$Q = (0, 0)$] is predicted.¹⁵⁻¹⁹ The FM J_1 - J_2 model with α in the range ~ 0.4 - 0.6 predicts either a spin nematic phase¹⁵ or a sharp phase boundary between FM order and collinear stripe order at $\alpha = 0.4$, i.e., no disorder phase exists at all.¹⁶ It is, therefore, evident that the observed magnetic ground state for

TABLE I. Irreducible representations of the group of the propagation vector $G_{\mathbf{k}}$.

Symmetry element of $G_{\mathbf{k}}$	1	2 (0, y, 0)	m(x, y, 0)	m(0, y, z)
Γ_1	1	1	1	1
Γ_2	1	1	-1	-1
Γ_3	1	-1	1	-1

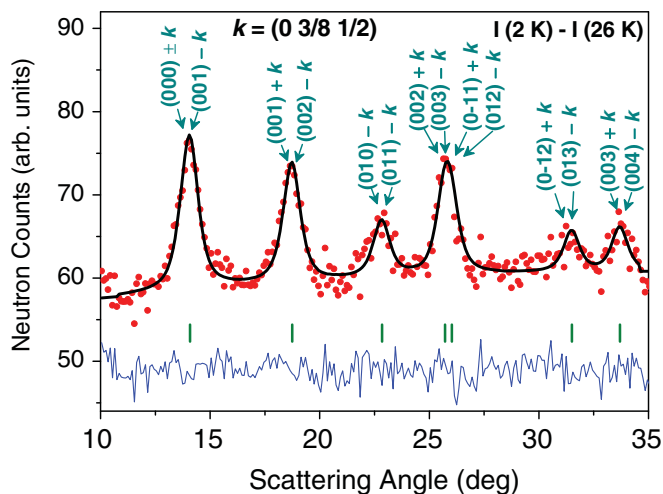


FIG. 4. (Color online) The fit of the magnetic diffraction profile calculated using the helical AFM structure to the 2 K difference pattern shown in Fig. 3. The vertical bars show the allowed magnetic Bragg peak positions according to the propagation vector $k = (0 \ 3/8 \ 1/2)$. The (hkl) values for the observed magnetic peaks are also listed.

the present system with $\alpha = 0.59$ does not match with the theoretical predictions and/or experimental reports for FM J_1 and AFM J_2 systems. The observed moment of $0.79(7) \mu_B$ at 2 K is typical for Cu^{2+} oxides, with some reduction from the ideal value of $1 \mu_B$ due to covalency effects and quantum fluctuations. For a pure 2D $S = 1/2$ AFM square-lattice system, the expected ordered magnetic moment is $\sim 0.6 \mu_B$ per ion.^{44,45}

It is therefore, evident that the magnetic ground state for the present system differs from the theoretical prediction with FM J_1 - J_2 model for a spin-1/2 Heisenberg square-lattice spin system. The observed AFM spiral structure is also different from experimentally reported results for other square-lattice spin systems with FM J_1 . However, we note that a helical-spiral AFM structure for a $S = 1/2$ square-lattice Heisenberg system is predicted by introducing a next-to-next-nearest-neighbor (NNNN) exchange interaction J_3 .⁴⁶⁻⁵² Here, the J_3 is considered between a magnetic atom and its second-nearest neighbor along the side of the square [defined by the vectors $(\pm 2, 0)$ or $(0, \pm 2)$] as shown in Fig. 2(b). In the J_1 - J_2 - J_3 model, four ordered magnetic ground states are predicted and disordered regions are likely in the vicinity of phase boundaries. The four ordered states are collinear and spiral states: (i) a AFM phase $Q = (\pi \ \pi)$ (for AFM J_1) or FM phase with $Q = (0 \ 0)$ (for FM J_1); (ii) a collinear phase with $Q = (\pi \ 0)$ or $(0 \ \pi)$ for both FM and AFM J_1 ; (iii) a spiral phase with $Q = (q \ \pi)$ or $(\pi \ q)$ for AFM J_1 , whereas, $Q = (q \ 0)$ or $(0 \ q)$ for FM J_1 , where $q = \cos^{-1}(-\frac{J_1+2J_2}{4J_3})$; and (iv) a spiral phase with $Q = (q \ q)$ or $(q \ -q)$ where $q = \cos^{-1}(-\frac{J_1}{2J_2+4J_3})$ for both FM and AFM J_1 . In the present case, we found the k vector $(0 \ 3/8)$, i.e., the third $Q = (0 \ q)$ type. The observed k vector $(0 \ 3/8)$ suggests a ferromagnetic J_1 as reported in the magnetization study.³² It is therefore, likely that J_3 is present for the studied compound. However, it requires an experimental confirmation. It is, therefore, necessary to perform further experiments, specially, an inelastic neutron scattering on single crystals of the present compound to measure J_1 , J_2 , and particularly J_3 .

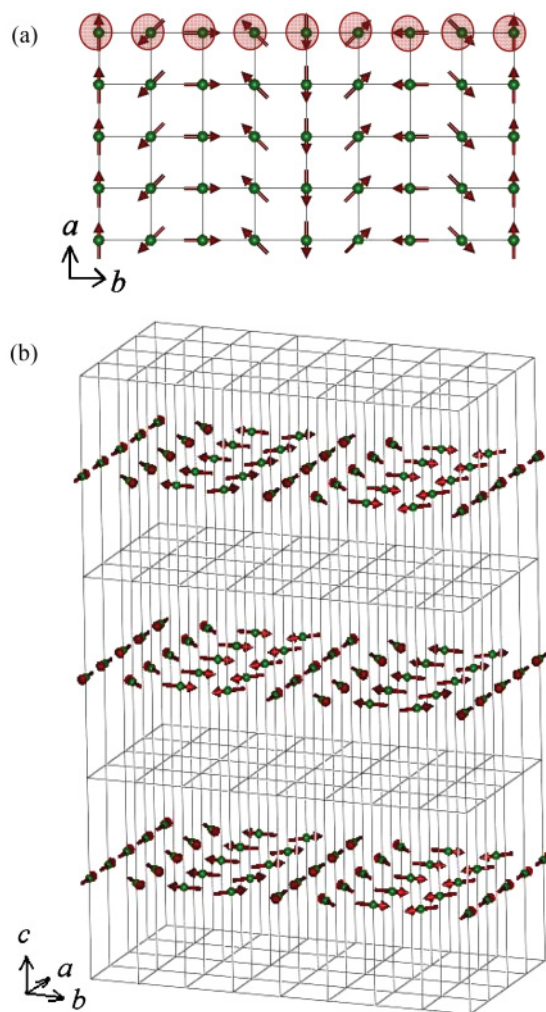


FIG. 5. (Color online) (a) The in-plane helical AFM structure of $(\text{CuBr})\text{Sr}_2\text{Nb}_3\text{O}_{10}$ showing Cu spins on a $4a \times 8b$ array. (b) The AFM coupling of helical planes along the c axis shown on a $4a \times 8b \times 3c$ array. (a , b , and c are nuclear unit cell parameters).

In order to understand the $1/3$ magnetization plateau in the $M(H)$ curve for $(\text{CuBr})\text{Sr}_2\text{Nb}_3\text{O}_{10}$, we have carried out a neutron diffraction study under an applied magnetic field of 4.5 T at 2 K. Figure 6 shows the magnetic diffraction patterns at 2 K and 4.5 T, after subtraction of the 12 K nuclear profile. Magnetic Bragg peaks appear at different scattering angles from those of the magnetic Bragg peaks under zero field (Figs. 3 and 4) confirming a second type of AFM structure under a magnetic field. All magnetic peaks can be indexed with an incommensurate propagation vector $k_1 = (0 \ 1/3 \ 0.446)$ and

TABLE II. Basis vectors of position $1b$ $(0, 0, 0.5)$ for the representations Γ_1 , Γ_2 , and Γ_3 .

Irreducible representations	Basis vectors	
Γ_1	Ψ_1	$(1 \ 0 \ 0)$
Γ_2	Ψ_1	$(0 \ 0 \ 1)$
Γ_3	Ψ_1	$(0 \ 1 \ 0)$

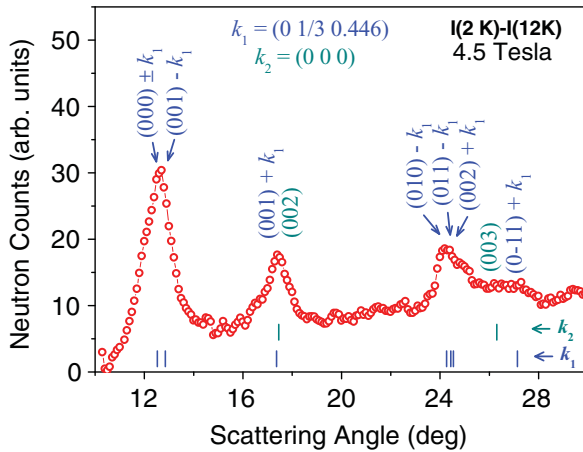


FIG. 6. (Color online) The magnetic diffraction pattern of $(\text{CuBr})\text{Sr}_2\text{Nb}_3\text{O}_{10}$ measured at 2 K under a 4.5 T magnetic field, after subtraction of the 12 K nuclear profile. The peaks are indexed with a propagation vector $k_1 = (0 \ 1/3 \ 0.446)$ and a probable $k_2 = (0 \ 0 \ 0)$ vector.

are mostly composed of several magnetic satellites as shown in Fig. 6.

The observation of magnetic order with the propagation vector $k_1 = (0 \ 1/3 \ 0.446)$ under a 4.5 T magnetic field provides a direct microscopic confirmation of a change of the magnetic structure at the $1/3$ magnetization plateau, which had been observed in the previous magnetization study.³² An in-plane magnetic structure with $Q = (0 \ 2\pi/3)$ was theoretically predicted from the quantization condition of the plateau magnetization.³² According to theoretical work by Oshikawa *et al.*⁵³ for a Heisenberg spin system, the quantization condition on the magnetization at a plateau is $p(S-m) = \text{integer}$, where p and m are the period of the spin state and the magnetization per site, respectively. For the present compound with $S = 1/2 \text{ Cu}^{2+}$ ions, the minimal necessary condition of the $1/3$ plateau ($m = 1/6$) gives the period as $p = 3$. $(\text{CuBr})\text{Sr}_2\text{Nb}_3\text{O}_{10}$ has only one Cu^{2+} ion per chemical unit cell which implies $p = 1$, so breaking of translational symmetry is needed to satisfy the quantization condition. Magnetic structures with an up-up-down arrangements of ferromagnetic chains (collinear AFM) in a given layer with propagation vectors $k = (0 \ 1/3)$ and $(1/3 \ 1/6)$ were proposed to explain the magnetization plateau.²⁸ Our neutron results do not confirm this prediction but confirm that within this field region the magnetic propagation vector is $k_1 = (0 \ 1/3$

$0.446)$ and has therefore completely changed as compared to the zero-field situation with $k = (0 \ 3/8 \ 1/2)$. In this respect our data support the existence of a different magnetic structure at the $1/3$ magnetization plateau. Apart from this purely antiferromagnetic propagation vector, the neutron data give indications of a very small ($0.25\text{--}0.35 \mu_B$) ferromagnetic contribution ($k_2 = (0 \ 0 \ 0)$) to the nuclear $(0 \ 0 \ 3)$ Bragg peak (Fig. 6). We do not attempt to present here quantitative fits to the powder diffraction data recorded under magnetic field as the limited number of detected magnetic Bragg peaks makes any refinement uncertain. Only a single crystal experiment will be able to solve the issue of the exact magnetic structure adopted within the $1/3$ magnetization plateau.

IV. SUMMARY AND CONCLUSIONS

In summary, a novel helical AFM structure has been found for the $S = 1/2$ square-lattice system $(\text{CuBr})\text{Sr}_2\text{Nb}_3\text{O}_{10}$ at temperatures below $T_N \sim 7.5$ K in its ground state. A helix of Cu spins is formed in the ab plane, and such planes are coupled antiferromagnetically along the c axis. The ordered moment is found to be $0.79(7) \mu_B/\text{Cu}^{2+}$ -ion at 2 K. The observed helical AFM structure is in contrast to the experimental observations and theoretical predictions for the ground state of a $S = 1/2$ square-lattice system on the basis of the J_1 - J_2 model. The observed helical magnetic ground state indicates that the third-nearest-neighbor exchange interaction J_3 may play a significant role for the present system. Under a 4.5 T magnetic field, we have observed a different magnetic structure, characterized by the propagation vector $k_1 = (0 \ 1/3 \ 0.446)$ and a probable $k_2 = (0 \ 0 \ 0)$ vector, which is different compared to the zero-field case.

ACKNOWLEDGMENTS

HK would like to acknowledge K. Totsuka, T. Momoi, and N. Shannon for useful discussion on the applicability of the J_1 - J_2 - J_3 model. This work was supported by Grants-in-Aid for Science Research in the Priority Areas “Novel States of Matter Induced by Frustration” (Grant No. 19052004) from the Ministry of Education, Culture, Sports, Science and Technology of Japan, the Global COE program International Center Science, Kyoto University, Japan, and by the Japan Society for the Promotion of Science (JSPS) through its “Funding Program for World-Leading Innovative R&D on Science and Technology (FIRST) Program”. JPA thanks EPSRC, STFC, and the Leverhulme Trust for support.

*Corresponding author: smyusuf@barc.gov.in

¹ L. J. de Jongh, *Magnetic Properties of Layered Transition Metal Oxide* (Kluwer Academic Publishers, Netherlands, 1990).

² G. Misguich and C. Lhuillier, in *Frustrated Spin Systems*, edited by H. T. Diep (World Scientific, Singapore, 2004), p. 229.

³ D. Schmalfuß, R. Darradi, J. Richter, J. Schulenburg, and D. Ihle, *Phys. Rev. Lett.* **97**, 157201 (2006).

⁴ P. Chandra and B. Doucot, *Phys. Rev. B* **38**, 9335 (1988).

⁵ E. Dagotto and A. Moreo, *Phys. Rev. Lett.* **63**, 2148 (1989).

⁶ F. Figueirido, A. Karlhede, S. Kivelson, S. Sondhi, M. Rocek, and D. S. Rokhsar, *Phys. Rev. B* **41**, 4619 (1990).

⁷ J. Richter, *Phys. Rev. B* **47**, 5794 (1993).

⁸ M. E. Zhitomirsky and K. Ueda, *Phys. Rev. B* **54**, 9007 (1996).

⁹ A. E. Trumper, L. O. Manuel, C. J. Gazza, and H. A. Ceccatto, *Phys. Rev. Lett.* **78**, 2216 (1997).

¹⁰ L. Siurakshina, D. Ihle, and R. Hayn, *Phys. Rev. B* **64**, 104406 (2001).

- ¹¹J. Sirker, Z. Weihong, O. P. Sushkov, and J. Oitmaa, *Phys. Rev. B* **73**, 184420 (2006).
- ¹²R. F. Bishop, P. H. Y. Li, R. Darradi, J. Schulenburg, and J. Richter, *Phys. Rev. B* **78**, 054412 (2008).
- ¹³J. Richter and J. Schulenburg, *Eur. Phys. J. B* **73**, 117 (2010).
- ¹⁴O. P. Sushkov, J. Oitmaa, and Zheng Weihong, *Phys. Rev. B* **63**, 104420 (2001).
- ¹⁵N. Shannon, T. Momoi, and P. Sindzingre, *Phys. Rev. Lett.* **96**, 027213 (2006).
- ¹⁶J. Richter, R. Darradi, J. Schulenburg, D. J. J. Farnell, and H. Rosner, *Phys. Rev. B* **81**, 174429 (2010).
- ¹⁷B. Schmidt, N. Shannon, and P. Thalmeier, *J. Phys.: Condens. Matter.* **19**, 145211 (2007).
- ¹⁸N. Shannon, B. Schmidt, K. Penc, and P. Thalmeier, *Eur. Phys. J. B* **38**, 599 (2004).
- ¹⁹P. Thalmeier, M. E. Zhitomirsky, B. Schmidt, and N. Shannon, *Phys. Rev. B* **77**, 104441 (2008).
- ²⁰R. Melzi, P. Carretta, A. Lascialfari, M. Mambrini, M. Troyer, P. Mittle, and F. Mila, *Phys. Rev. Lett.* **85**, 1318 (2000).
- ²¹N. Tsyrlin, T. Pardini, R. R. P. Singh, F. Xiao, P. Link, A. Schneidewind, A. Hiess, C. P. Landee, M. M. Turnbull, and M. Kenzelmann, *Phys. Rev. Lett.* **102**, 197201 (2009).
- ²²A. Bombardi, L. C. Chapon, I. Margiolaki, C. Mazzoli, S. Gonthier, F. Duc, and P. G. Radaelli, *Phys. Rev. B* **71**, 220406(R) (2005).
- ²³A. A. Tsirlin, A. A. Belik, R. V. Shpanchenko, E. V. Antipov, E. Takayama-Muromachi, and H. Rosner, *Phys. Rev. B* **77**, 092402 (2008).
- ²⁴K. Oka, I. Yamada, M. Azuma, S. Takeshita, K. H. Satoh, A. Koda, R. Kadono, M. Takano, and Y. Shimakawa, *Inorg. Chem.* **47**, 7355 (2008).
- ²⁵N. S. Kini, E. E. Kaul, and C. Geibel, *J. Phys.: Condens. Matter.* **18**, 1303 (2006).
- ²⁶S. M. Yusuf, A. K. Bera, N. S. Kini, I. Mirebeau, and S. Petit, *Phys. Rev. B* **82**, 094412 (2010).
- ²⁷E. E. Kaul, H. Rosner, N. Shannon, R. V. Shpanchenko, and C. Geibel, *J. Magn. Magn. Mater.* **272–276**, 922 (2004).
- ²⁸L. Bossoni, P. Carretta, R. Nath, M. Moscardini, M. Baenitz, and C. Geibel, *Phys. Rev. B* **83**, 014412 (2011).
- ²⁹E. E. Kaul, Ph.D. dissertation, Technical University Dresden, 2005.
- ³⁰R. Nath, A. A. Tsirlin, H. Rosner, and C. Geibel, *Phys. Rev. B* **78**, 064422 (2008).
- ³¹A. A. Tsirlin, R. Nath, A. M. Abakumov, R. V. Shpanchenko, C. Geibel, and H. Rosner, *Phys. Rev. B* **81**, 174424 (2010).
- ³²Y. Tsujimoto, Y. Baba, N. Oba, H. Kageyama, T. Fukui, Y. Narumi, K. Kindo, T. Saito, M. Takano, Y. Ajiro, and K. Yoshimura, *J. Phys. Soc. Jpn.* **76**, 063711 (2007).
- ³³Y. Tsujimoto, H. Kageyama, Y. Baba, A. Kitada, T. Yamamoto, Y. Narumi, K. Kindo, M. Nishi, J. P. Carlo, A. A. Aczel, T. J. Williams, T. Goko, G. M. Luke, Y. J. Uemura, Y. Ueda, Y. Ajiro, and K. Yoshimura, *Phys. Rev. B* **78**, 214410 (2008).
- ³⁴T. A. Kodenkandath, J. N. Lalena, W. L. Zhou, E. E. Carpenter, C. Sangregorio, A. U. Falster, Jr. W. B. Simmons, Charles J. O'Connor, and J. B. Wiley, *J. Am. Chem. Soc.* **121**, 10743 (1999).
- ³⁵T. A. Kodenkandath, A. S. Kumbhar, W. L. Zhou, and J. B. Wiley, *Inorg. Chem.* **40**, 710 (2001).
- ³⁶H. Kageyama, T. Kitano, R. Nakanishi, J. Yasuda, N. Oba, Y. Baba, M. Nishi, Y. Ueda, Y. Ajiro, and K. Yoshimura, *Prog. Theor. Phys. Suppl.* **159**, 39 (2005).
- ³⁷J. Rodriguez-Carvajal, *Physica B* **192**, 55 (1993).
- ³⁸FullProf Suite [<http://www.ill.eu/sites/fullprof/>].
- ³⁹C. Tassel, J. Kang, C. Lee, O. Hernandez, Y. Qiu, W. Paulus, E. Collet, B. Lake, T. Guidi, M.-H. Whangbo, C. Ritter, H. Kageyama, and S.-H. Lee, *Phys. Rev. Lett.* **105**, 167205 (2010).
- ⁴⁰A. A. Tsirlin, A. M. Abakumov, G. Van Tendeloo, and H. Rosner, *Phys. Rev. B* **82**, 054107 (2010).
- ⁴¹E. F. Bertaut, in *Magnetism III*, edited by G. T. Rado and H. Suhl (Academic Press, New York, 1963), p. 149.
- ⁴²E. F. Bertaut, *Acta Crystallogr. Sec. A* **24**, 217 (1968).
- ⁴³N. Oba, H. Kageyama, T. Kitano, J. Yasuda, Y. Baba, M. Nishi, K. Hirota, Y. Narumi, M. Hagiwara, K. Kindo, T. Saito, Y. Ajiro, and K. Yoshimura, *J. Phys. Soc. Jpn.* **75**, 113601 (2006).
- ⁴⁴E. Manousakis, *Rev. Mod. Phys.* **63**, 1 (1991).
- ⁴⁵B. G. Liu, *Phys. Rev. B* **41**, 9563 (1990).
- ⁴⁶I. G. Gochev, *Phys. Rev. B* **51**, 16421 (1995).
- ⁴⁷M. P. Gelfend, R. R. P. Singh, and David A. Huse, *Phys. Rev. B* **40**, 10801 (1989).
- ⁴⁸M. Mambrini, A. Läuchli, D. Poilblanc, and F. Mila, *Phys. Rev. B* **74**, 144422 (2006).
- ⁴⁹A. Moreo, E. Dagotto, Th. Jolicoeur, and J. Riera, *Phys. Rev. B* **42**, 6283 (1990).
- ⁵⁰A. Chubukov, *Phys. Rev. B* **44**, 392 (1991).
- ⁵¹J. Ferrer, *Phys. Rev. B* **47**, 8769 (1993).
- ⁵²P. Sindzingre, L. Seabra, N. Shannon, and T. Momoi, *J. Phys.: Conf. Ser.* **145**, 012048 (2009).
- ⁵³M. Oshikawa, M. Yamanaka, and I. Affleck, *Phys. Rev. Lett.* **78**, 1984 (1997).